THE JOURNAL OF PHYSICAL CHEMISTRY Letters

Physical Insights into Energy Science

The Effect of the Perovskite Thickness on the Electroluminescence and Solar Cell Conversion Efficiency

Monika Rai, Lydia H. Wong, and Lioz Etgar

J. Phys. Chem. Lett., **Just Accepted Manuscript** • DOI: 10.1021/acs.jpclett.0c02363 • Publication Date (Web): 07 Sep 2020

Effect of Perovskite Thickness on Electroluminescence and Solar Cell Conversion Efficiency

Monika Rai[a,b], Lydia Helena Wong[a,b,*] , Lioz Etgar[a,c,*]

[a]Campus for Research Excellence and Technological Enterprise (CREATE), 1 Create Way, 138602, Singapore

[b]School of Material Science and Engineering, Nanyang Technological University, 639798 Singapore, Singapore

[c]The Hebrew University of Jerusalem, Institute of Chemistry, Casali Center for Applied Chemistry, Jerusalem 91904, Israel

* lioz.etgar@mail.huji.ac.il, LydiaWong@ntu.edu.sg

Abstract:

A hybrid organic–inorganic perovskite in a diode structure can lead to multifunctional device phenomena exhibiting both a high-power conversion efficiency (PCE) of a solar cell and strong electroluminescence (EL) efficiency. Non radiative losses in such multifunctional devices lead to open circuit voltage (V_{oc}) deficit which is a limiting factor to push the efficiency towards Shockley–Queisser (SQ) limit. In this work we analyse and quantify the radiative limit of V_{oc} in perovskite solar cell as a function of its absorber thickness. We correlate PCE and EL efficiency at varying thicknesses to understand the limiting factors for high V_{oc}. With certain increase in perovskite thickness, PCE improves but EL efficiency is compromised and, vice versa. Thus, correlating these two figures of merits of a solar cell guides towards light management strategy together with minimizing non-radiative losses. The results demonstrate that maximizing absorption and emission processes remains paramount for optimizing devices.

TOC image:

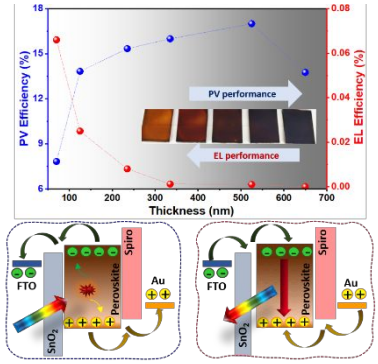

Over the past few years, the performance of lead halide based perovskite solar cells (PSCs) have revolutionized the photovoltaic field.[1-5] Their strong absorption bands spanning the visible region and excellent charge transport properties together with low cost solution processability make them ideal candidates for both photovoltaic (PV) devices and light emitting diodes (LEDs).[6, 7] Although the current power conversion efficiency (PCE) of ca. 25% is remarkable, the open-circuit voltage (V_{oc}) of these solar cells remains below their theoretical V_{OC} limit of 1.32 V (corresponding to 1.6 eV band gap, common to lead halide perovskites) at AM 1.5 G sunlight.[8, 9] This loss arises from nonradiative recombination of photogenerated charge carriers which demands for a quantification and identification of the dominating recombination mechanisms.[10] Under a generalized Shockley–Queisser (SQ)-approach, Uwe Rau proposed an opto-electronic reciprocity theorem between absorption and emission. Thus, a solar cell that has theoretical maximum PCE will also give maximum external quantum efficiency (EQE) of its electroluminescence (EQE_{EL} %) emission.[11] There are few reports with high EL efficiency corresponding to high efficiency devices but their still exists enormous scope to maximize the emission.[10, 12] Moreover, it is a daunting task to prepare a device which exhibit high PV performance and excellent EQE_{EL} at the same time.[13] But, the key lies in maximizing absorption and emission processes for optimizing high efficiency devices.

Owing to the occurrence of non-radiative losses due to defects, traps, geometrical loss (like reflection, waveguiding etc.) or other reasons in any real PV system, the EQE_{EL} is less than 1. Therefore, the experimentally observed V_{OC} values of solar cells are lower than the actual radiative limit and are given by: [4, 13, 14]

$$\boldsymbol{V_{oc}^{Cell} = V_{oc}^{Rad} - \frac{kT}{q}|\ln EQE_{EL}|} \quad (1)$$

where V_{oc}^{Cell} is the calculated V_{OC} of the solar cell and V_{oc}^{Rad} is the radiative limit. This reciprocity relation suggests that a higher EQE_{EL} results in a higher V_{oc}. Thus, although the physical mechanism of a solar cell (radiation energy into electricity) and EL (transformation of electrical energy into light) is different, the attainable V_{oc} is related by virtue of equation 1. [13, 15] In this work, we use equation 1 to probe V_{oc} deficit in $Cs_{0.2}FA_{0.8}Pb(I_{0.85}Br_{0.15})_3$ based PSC by varying perovskite thickness. The evaluation of Voc from equation 1 was first attempted in $MAPbI_3$ PSC [16, 17] Whereas for a good PV device, a significant thickness is required to get enough light absorption and efficient charge carrier collection, its high EQE_{EL} requires minimum thickness to reduce waveguiding loss and quenching of EL emission.[18] Importantly, our objective is not to optimise the device structure for the best performance of PSC or EL emission. Instead, we aim to study the correlation between PCE and EL efficiency as a function

of absorber thickness. To probe the non-radiative losses in the photo absorber we only vary perovskite thickness keeping other layers and deposition technique the same. If perovskite is sufficiently thick (in the range of its absorption coefficient)[19] then it leads to an excellent PV performance with enough current density produced. However, EL performance at this thickness is often compromised as photons that are emitted internally are likely to be trapped or re-absorbed (matching emission and absorption energy). This limits the luminescence yield and hence the V_{oc} value. Herein, we fabricate high performance MA free perovskite ($Cs_{0.2}FA_{0.8}Pb(I_{0.85}Br_{0.15})_3$) with a stable and well-studied composition [20, 21] solar cells with a planar structure (n-i-p) using single step method, and carefully elucidate the effect of its thickness, morphology and transparency on the PCE and EL performance and illustrate how it defines the inherent losses. These two reciprocal device operations suggest a way to quantify the absorber quality and, to minimize defects in the bulk absorber.

Figure 1 illustrates the working mechanism of EL in a LED and PV together with the energy level scheme for perovskite in n-i-p structure. In EL, charges are injected through respective charge transport layers (i.e. in forward bias) into the perovskite where they recombine to give bright Near-Infra-Red (NIR) emission. In PV device, the identical stack is put under 1 Sun illumination where electron hole pairs are generated by absorbing light. The generated electrons are extracted by SnO_2 layer (ETL) and holes by Spiro-OMETAD (HTL) due to their suitable band matching, respectively. The PV device operates in both forward and reverse bias.

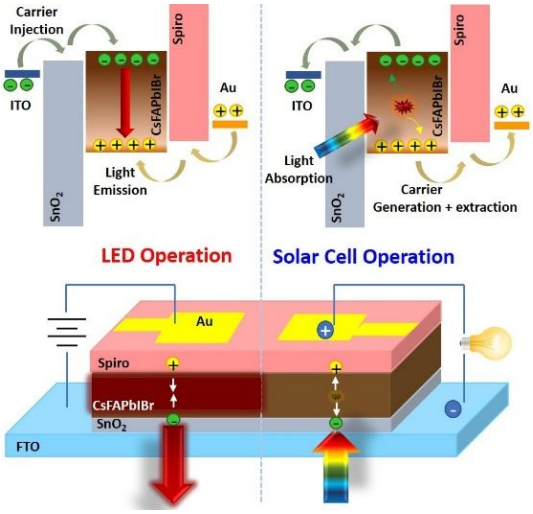

Figure 1: Schematic representation of Perovskite LED and solar cell operation with energy level diagrams showing recombination in the LED and carrier extraction in the solar cell.

Ideally, for the best EL performance, EQE_{EL} is ~1. In that case, from **equation 1,** we get $V_{oc}^{cell} \sim V_{oc}^{Rad}$ and hence we approach the radiative limit of the V_{oc} for a solar cell if the device stack is the same. However, to make such device which is equally good in both operations

simultaneously is neither trivial nor straightforward. The perovskite is a defect tolerant material with low trap density and most of the radiative recombination happens through band to band transition.[22, 23]

Figure 2(a) shows statistical distribution of the PCE at different concentration of the perovskite solution. The perovskite precursor solution concentration (in molarity, M) is the direct translation of the absorber thickness as shown at the inset of figure 2(a). The thickness varies from 70 nm for 0.4 M to 630 nm for 1.4 M as deduced from figure S1 which shows the SEM (Scanning Electron Microscopy) cross section of a series of devices.

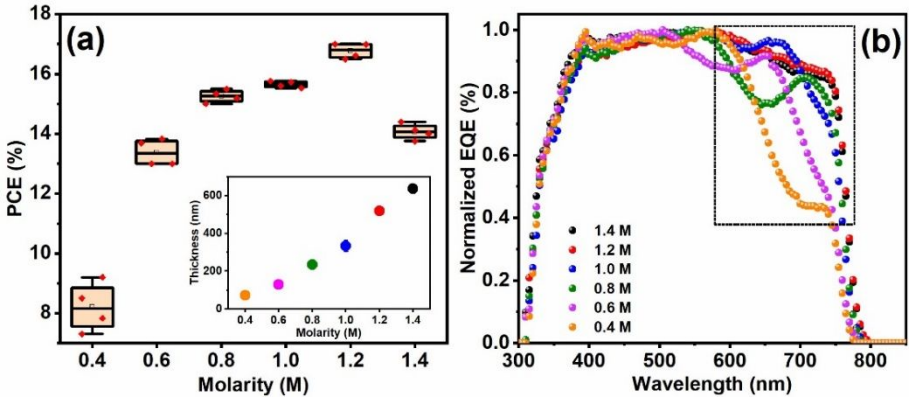

Figure 2: (a) Statistical distribution of PV performance of perovskite solar cells at different concentration. Inset- the perovskite thickness as a function of the concentration. (b) the corresponding EQE spectra.

The rest of the PV parameters are shown in figure S3. There is a continuous rise in J_{sc} with increasing thickness approaching a saturation at 22 mA/cm^2 for 1.4 M perovskite. Clearly, the thickness of the absorber is a key parameter for optimal carrier generation. However, crystal quality also plays a significant role in avoiding non radiative losses of photogenerated carriers due to grain boundaries or other defects in the lattice. The role of high-quality absorber specially becomes significant at low thickness where carrier generation is already low. Figure S2 shows smaller grain size for thinner perovskite layer affecting the electric properties of the material like generation, transport and collection of photogenerated carriers. For thinner perovskite, lesser precursor solution is left for nucleated particles to grow, hence smaller grain size. With increasing concentration of perovskite, the Ostwald ripening predominates resulting in large grain growth.

For thicker devices, most of the light harvested by the perovskite contributes to the current. The PCE has a Similar trend except that it drops at 1.4 M, as a result of sudden decrease in V_{oc} and FF due to too thick perovskite layer causing aggravated recombination loss.[24] Figure 2(b) shows the normalized external quantum efficiency (EQE_{PV}) of the PV devices showing that the loss in J_{sc} occurs mainly at higher wavelength (> 600 nm). This is expected due to the

wavelength dependent absorption coefficient of perovskite (see fig S4). The absorption reduces for thin perovskite which affects photogeneration specially at higher wavelengths. No significant change in band edge absorption is observed. Thus, we expect the same radiative limit of V_{oc} for all the devices.

The optical band gap is further calculated from the Tauc plot. Figure S4(a) shows the UV-Vis absorption spectroscopy of perovskite films on SnO_2 substrates showing the signature peak of perovskite at 730-770 nm. The average visible transparency (AVT) reduces with increasing concentration which is summarized at the inset of figure S4(a). Whereas low AVT is required for high EQE_{PV} as most of the absorbed light contributes to photogenerated current, one needs high AVT for EQE_{EL} as it effectively suppresses waveguiding and improves light outcoupling. Due to the high refractive index of the perovskite (≈2.3 near the emission wavelength), waveguiding mode loss is a major loss channel for perovskite and strongly dependent on the thickness of the perovskite layer.[25] Thus, if one is interested in semi-transparent PSC specifically for window applications (AVT ~ 25-35%), these losses are, by default, controlled. [21] With increasing thickness, therefore, it becomes essential to control it with interfacial texturing to enhance light trapping which would generate higher number of charge carriers and hence higher J_{sc}. Figure S4(b) shows the optical band gap of the perovskite equal to ~1.62eV in agreement with figure 2(b). The (X Ray Diffraction pattern) XRD in Fig S5 confirms the cubic phase of the perovskite for different thicknesses[26].

Next, EL measurement was carried out on the same set of PV devices with different thicknesses by charge carrier injection method. In the case of EL mechanism, charge carriers are injected through the respective ETL and HTL layers in forward bias. [27] Fig 3(a)-(e) shows the current density and EL radiance behaviour with respect to applied voltage. There is no EL performance observed for 1.4 M film which can be attributed to the compromised absorber quality and complete quenching. We suspect that Joule heating could also be the reason where thicker perovskite layer forms a stronger barrier for efficient thermal dissipation leading to elevated junction temperature.[25]

For all the concentrations, the onset of EL emission is ~ 1 V which is close to the Voc. The plateau region of the EL radiance contracts continuously from 0.4 to 1.2 M with reduction in its absolute value. This suggests that both EL efficiency and stability decrease as thickness increases. A possible explanation is the large portion of the input power that gets converted to heat or self-quenching of EL emission. Also, EL degradation is faster for devices with a thicker perovskite layer which support the heat generation/accumulation mechanism. A comparison of

relative intensity of EL spectra is shown in Fig 3 (f) at a constant applied bias of 3 V (which is mostly the plateau region of radiance).

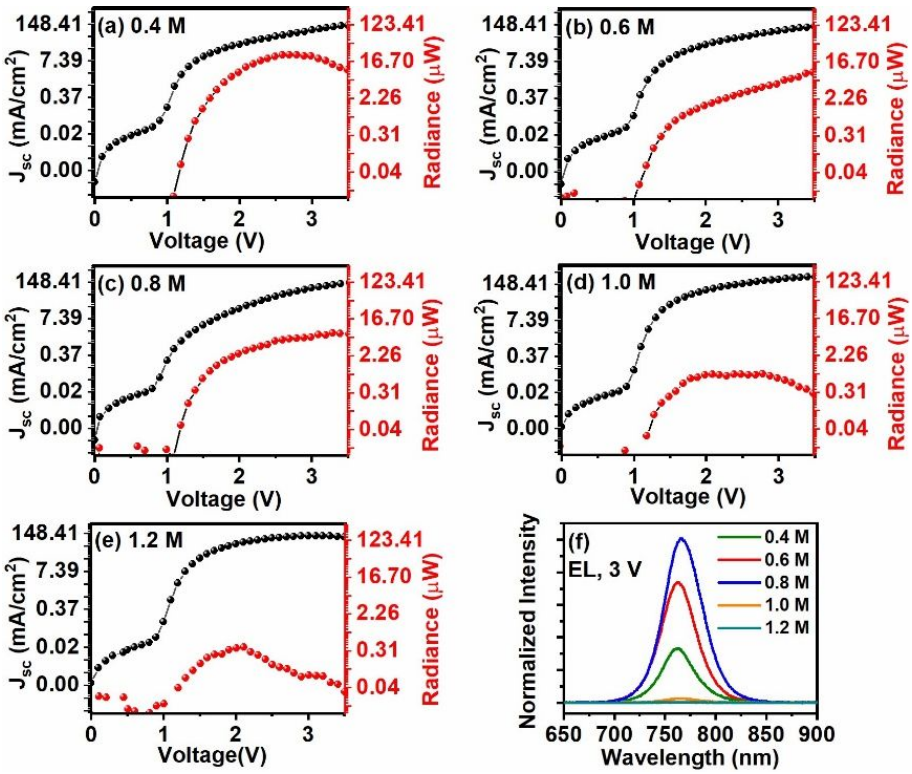

Figure 3. (a) - (e) Current Density-Voltage (J-V) (blacks dots) and Radiance -Voltage (red dots) curves and (f) EL spectra at 3 V applied bias, for different concentrations.

The EL intensity increases from 0.4 M to 0.8 M and thereafter decreases. Although we have maximum EL emission for 0.8 M, we don't have maximum radiance for the same. This is limited by high carrier injection as shown in Fig 4 (a). EL emission intensity alone does not guarantee to get a good LED. Therefore, the EL performance is maximum when we have both, low injection current and high radiative efficiency.

In order to analyse the effect of thickness on the film quality we performed photoluminescence (PL) measurements. The increase in film quality with thickness is corroborated with improved PL performance (see Fig S6) in terms of reduced FWHM (full width at half maxima) and PL maxima shifting to lower wavelength due to the reduction in grain boundaries (see fig S2).[28] The time resolved PL (TRPL) measurements presented in fig S6 (d) shows faster carrier decay for 1.2 M device as compared to 0.4 M. This can be attributed to various decay channels like bimolecular recombination, trapping, charge extraction etc. which is subject to investigation (but beyond the scope of this study). For simplicity, as perovskite is coated on ETL it is equivalent to short circuit condition in PL [29], the fast decay can arise due to rapid charge carrier transport from the perovskite to the ETL layer. Whereas this sharp decay is beneficial for PV performance in terms of fast extraction of photogenerated carriers, it inhibits the recombination

mechanism in EL measurement. Fig. S7 further shows the EL and PL spectra plotted together where there is an absolute overlap in the case of 0.4 and 0.6 M but it starts to diverge for higher concentration. EL maxima remains same whereas PL maxima blue shifts. The EL spectra for individual concentration at varying applied bias is shown in Fig S8.

Fig 4(a) shows the variation of carrier density [current density/ (elementary charge× thickness)] with varying voltage for different concentration. It suggests that the voltage requirement to get essentially the same carrier density increases with thickness of the perovskite (as shown by the vertical grey dotted lines corresponding to carrier density of $2x10^{25}$ cm^{-3}). For a good EL emission, the carrier injection should happen at minimum applied bias. The bias increases with the absorber thickness as the spatial distribution of injected carriers offers resistance towards recombination. [30 31]

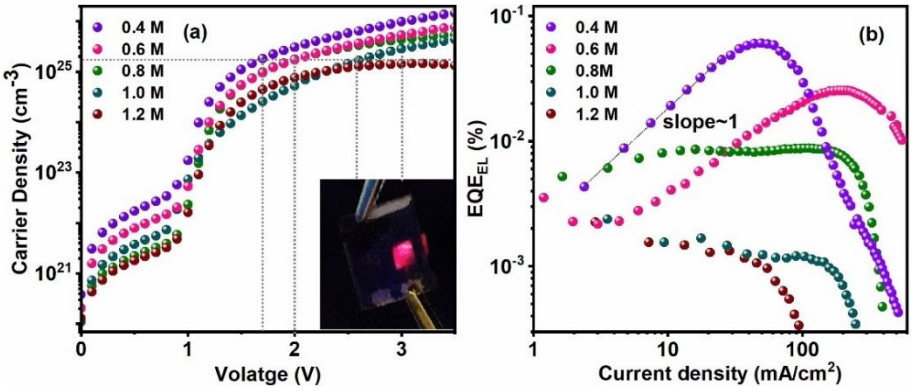

Figure 4. (a) Variation of carrier density with applied voltage at different concentration/thickness of perovskite. Inset shows the EL image of the device, (b) EQE of LED devices plotted as a function of current density for different thicknesses. The black dotted line shows straight line fit for 0.4 M ($\chi^2 \sim 0.999$)

Fig 4(b) shows the EQE_{EL} with respect to the injected current density for devices with different concentration. By plotting ln (EQE_{EL}) as a function of the ln J_{inj} (injection current), it is possible to determine the ideality factor (**n**) of the device.[32] If we compare following equation,

$$V_{oc}^{cal} = \frac{kT}{q}\ln\left(\frac{J_{sc}}{J_o^{Rad}}\right) - \frac{kT}{q}\ln\left(EQE_{EL}\right) = n\frac{kT}{q}\ln\left(\frac{J_{sc}}{J_o}\right) \quad (2)$$

where **n** is ideality factor, and EQE_{EL} a function of injection current, we see that for **n=1**, the EQE_{EL} should be constant, whereas it should increase linearly with injection current for **n=2**.[33] For 0.4 M device, the slope is 1. i.e. EQE_{EL} increases linearly with injection current indicating that much of the recombination happens through defects/ trap assisted non radiative recombination (Shockley-Read-Hall (SRH)). Thus, occurrence of SRH recombination suggests that **n=2** and for low thickness absorbers it can be attributed to shallow or surface defects originating from low surface to volume ratio of the grains (see Fig S2). [34 35] With increasing thickness, EQE_{EL} becomes constant i.e. **n ≈ 1** implying band-to-band recombination. Thus, whereas the EL is strong and stable in thin absorbers, it has non radiative decay channels due

to grain boundaries defects. As the thickness increases to optimum values, EL performance goes down, but most of the recombination is radiative suggesting lower defects. These counter behaviours largely affect the photovoltage values and therefore maximizing the EQE_{EL} is the key. Table 1 shows the values of V_{oc}, J_{sc} and EQE_{EL} values for each concentration where the injection current equals to the photocurrent (J_{sc}, measured at 1 Sun). The value of the dark current (J_o) is calculated using the equation [17]:

$$\boldsymbol{J_o} = \left(\frac{\boldsymbol{J_{sc}}}{\exp\left(\frac{\boldsymbol{V_{oc}}}{\boldsymbol{kT/q}}\right)}\right) \quad (3)$$

Followed by calculating the dark saturation current ($\boldsymbol{J_o^{Rad}}$) in the radiative limit:

$$\boldsymbol{J_o^{Rad}} = \boldsymbol{J_o}.\,\boldsymbol{EQE_{EL}} \quad (4)$$

Finally, $\boldsymbol{V_{oc}^{Rad}}$ and $\boldsymbol{V_{oc}^{non-Rad}}$ are calculated using:

$$\boldsymbol{V_{oc}^{Rad}} = \frac{\boldsymbol{kT}}{\boldsymbol{q}}\ln\left(\frac{\boldsymbol{J_{sc}}}{\boldsymbol{J_o^{Rad}}}\right),\ \boldsymbol{V_{oc}^{non-Rad}} = \frac{\boldsymbol{kT}}{\boldsymbol{q}}\ln|\mathbf{EQE_{EL}}| \quad (5)$$

At last, using equation 1, the calculated V_{oc} ($\boldsymbol{V_{oc}^{Cell}} = \boldsymbol{V_{oc}^{Rad}} - \boldsymbol{V_{oc}^{non-Rad}}$) is derived.

Table 1. Tabulated values of Concentration (M) and device parameters J_{sc} (mA/cm^2) and V_{oc} (V), calculated J_o, EQE_{EL}, calculated J_o^{Rad}, calculated V_o^{Rad}, calculated $V_o^{non-Rad}$ and calculated V_{oc}^{cell}.

Conc. (M)	J_{sc} (mA/cm^2)	V_{oc} (V)	J_o (mA/cm^2)	EQE_{EL} (%)	J_o^{Rad} (mA/cm^2)	V_{oc}^{Rad} (V)	$V_{oc}^{non-Rad}$ (V)	V_{oc}^{Cell} (V)
1.2	21.6	1.03	1.09E-16	0.001	1.09E-19	1.209	0.178	1.031
1.0	21	1.04	7.18E-17	0.002	1.44E-19	1.201	0.16	1.041
0.8	20	1.04	6.84E-17	0.007	4.79E-19	1.170	0.128	1.040
0.6	17.5	1.09	8.66E-18	0.008	6.93E-20	1.215	0.125	1.089
0.4	12	1.09	5.94E-18	0.04	2.38E-19	1.173	0.083	1.090

We now see that $\boldsymbol{V_{oc}^{Rad}}$ is ~1.2 V for our device and the calculated V_{oc} matches with the measured V_{oc}. Although $\boldsymbol{V_{oc}^{Rad}}$ is lower in our case as compared to reported literature[17], but being a device property, it relies on how good the device is made and measurements are performed. Clearly, V_{oc}^{cell} is closer to the radiative limit for thinner devices.

Figure 5 shows the link between the PV and the EL performance as suggested by equation 1. Figure 5(a) shows that the V_{oc} deficit (ΔV_{oc}= $\boldsymbol{V_{oc}^{non-Rad}}$) increases with concentration. In other words, it is a measure of non-radiative losses leading to V_{oc} deficit that shows increment with thickness. In figure 5(b), the PV performance improves whereas EL performance decreases within a range of increasing concentration. The major improvement in PCE comes from the current density which is primarily a function of the absorber thickness. Whereas, EQE_{EL} improves if we have sufficiently thin absorber to overcome luminescence quenching. Absorber

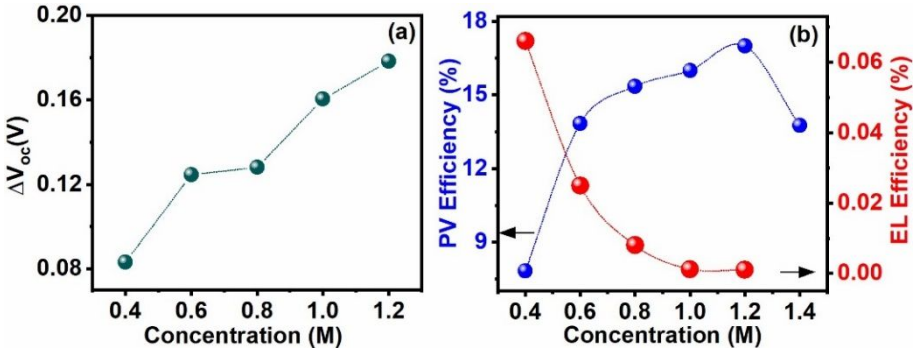

Figure 5. (a) V_{oc} deficit (ΔV_{oc}) as a function of concentration. (b) A comparison of PV and LED efficiency with concentration of the perovskite layer.

thickness is one common factor that collectively affects these two functionalities.

In conclusion, we used the same n-i-p device stack to study the PV and the EL behaviour. In order to do that we vary the perovskite thickness and follow the V_{oc} deficit which determine the overall efficiency. Moreover, we analysed the loss in the experimental V_{oc} measured from the PV as compared to the V_{oc} estimated from the EL. Clearly, thickness brings in major loss mechanisms which decreases the EQE_{EL}. SRH recombination and insufficient photogeneration of carriers limit PV performance of thinner device. For thicker device, high carrier injection requirement to get EL limits device stability and accelerates degradation pathways. We conclude that to maximize PCE and EL efficiency, one must maximize absorptance and emittance. This can be done by quantifying the achievable V_{oc} and improve the absorber accordingly. In the case of thin PSCs that shows strong EL but poor current density, photon management/concentration strategy can be adopted to overcome carrier limitation. Non radiative recombination can be mitigated via passivation of defects, particularly at grain boundaries and interfaces. For standard thicknesses with high PV efficiency but compromised EL, device texturing can be beneficial to limit the optical losses.

Supporting Information

Experimental procedure for device fabrication and details of characterizations, SEM images, device performance, transmittance data, XRD measurements, PL, TRPL and EL measurements

Author Information

The authors declare no competing financial interests.

Author Contributions: L.E. and M.R. conceived and planned the work. M.R. executed the experiments and wrote first version of the manuscript. L.H.W, L.E. finalized the manuscript.

Acknowledgements

This research is supported by the National Research Foundation, Prime Minister's Office, Singapore, through the Singapore-HUJ Alliance for Research and Enterprise (SHARE) and Nanomaterials for Energy and Water Management (NEW), NEW-CREATE Phase programme.

References:

(1) Pazos-Outón, L. M.; Xiao, T. P.; Yablonovitch, E. Fundamental Efficiency Limit of Lead Iodide Perovskite Solar Cells. *J. Phys. Chem. Lett.* **2018**, *9* (7), 1703-1711.

(2) Gao, P.; Grätzel, M.; Nazeeruddin, M. K. Organohalide Lead Perovskites for Photovoltaic Applications. *Energy Environ. Sci.* **2014**, *7* (8), 2448-2463.

(3) Snaith, H. J. Perovskites: The Emergence of a New Era for Low-Cost, High-Efficiency Solar Cells. *J. Phys. Chem. Lett.* **2013**, *4* (21), 3623-3630.

(4) Nayak, P. K.; Mahesh, S.; Snaith, H. J.; Cahen, D. Photovoltaic Solar Cell Technologies: Analysing The State of The Art. *Nat. Rev. Mater.* **2019**, *4* (4), 269-285.

(5) Park, N.-G. Organometal Perovskite Light Absorbers Toward a 20% Efficiency Low-Cost Solid-State Mesoscopic Solar Cell. *J. Phys. Chem. Lett.* **2013**, *4* (15), 2423-2429.

(6) Quan, L. N.; García de Arquer, F. P.; Sabatini, R. P.; Sargent, E. H. Perovskites for Light Emission. *Adv. Mater.* **2018**, *30* (45), 1801996.

(7) Sum, T. C.; Mathews, N. Advancements in Perovskite Solar Cells: Photophysics Behind The Photovoltaics. *Energy Environ. Sci.* **2014**, *7* (8), 2518-2534.

(8) NREL Best Research-Cell Efficiency Chart. **2020**.

(9) Rühle, S. Tabulated Values of The Shockley–Queisser Limit for Single Junction Solar Cells. *Sol. Energy.* **2016**, *130*, 139-147.

(10) Bi, D.; Tress, W.; Dar, M. I.; Gao, P.; Luo, J.; Renevier, C.; Schenk, K.; Abate, A.; Giordano, F.; Correa Baena, J.-P. *et al.* Efficient Luminescent Solar Cells Based on Tailored Mixed-Cation Perovskites. *Sci. Adv.* **2016**, *2* (1), e1501170.

(11) Rau, U. Reciprocity Relation Between Photovoltaic Quantum Efficiency and Electroluminescent Emission of Solar Cells. *Phys. Rev. B.* **2007**, *76* (8), 085303.

(12) Tavakoli, M. M.; Tress, W.; Milić, J. V.; Kubicki, D.; Emsley, L.; Grätzel, M. Addition of Adamantylammonium Iodide to Hole Transport Layers Enables Highly Efficient and Electroluminescent Perovskite Solar Cells. *Energy Environ. Sci.* **2018**, *11* (11), 3310-3320.

(13) Yablonovitch, E.; Miller, O. D.; Kurtz, S. R. A Great Solar Cell Also Needs to be A Great LED: External Fluorescence Leads to New Efficiency Record. *AIP Conf. Proc.* **2013**, *1519* (1), 9-11.

(14) Ross, R. T. Some Thermodynamics of Photochemical Systems. *J. Chem. Phys.* **1967**, *46* (12), 4590-4593.

(15) Green, M. Radiative Efficiency of State-Of-The-Art Photovoltaic Cells. *Prog. Photovolt: Res. Appl.* **2012**, *20*, 472-476.

(16) Tress, W.; Marinova, N.; Inganäs, O.; Nazeeruddin, M. K.; Zakeeruddin, S. M.; Graetzel, M. Predicting the Open-Circuit Voltage of $CH_3NH_3PbI_3$ Perovskite Solar Cells Using Electroluminescence and Photovoltaic Quantum Efficiency Spectra: The Role of Radiative and Non-Radiative Recombination. *Adv. Energy Mater.* **2015**, *5* (3), 1400812.

(17) Tvingstedt, K.; Malinkiewicz, O.; Baumann, A.; Deibel, C.; Snaith, H. J.; Dyakonov, V.; Bolink, H. J. Radiative Efficiency of Lead Iodide Based Perovskite Solar Cells. *Sci. Rep.* **2014**, *4* (1), 6071.

(18) Liu, D.; Gangishetty, M. K.; Kelly, T. L. Effect Of $CH_3NH_3PbI_3$ Thickness on Device Efficiency in Planar Heterojunction Perovskite Solar Cells. *J. Mater. Chem. A.* **2014,** *2* (46), 19873-19881.

(19) Stranks, S. D.; Eperon, G. E.; Grancini, G.; Menelaou, C.; Alcocer, M. J.; Leijtens, T.; Herz, L. M.; Petrozza, A.; Snaith, H. J. Electron-Hole Diffusion Lengths Exceeding 1 Micrometer in an Organometal Trihalide Perovskite Absorber. *Science.* **2013**, *342* (6156), 341-344.

(20) Rehman, W.; McMeekin, D. P.; Patel, J. B.; Milot, R. L.; Johnston, M. B.; Snaith, H. J.; Herz, L. M. Photovoltaic Mixed-Cation Lead Mixed-Halide Perovskites: Links Between Crystallinity, Photo-Stability And Electronic Properties. *Energy Environ. Sci.* **2017**, *10* (1), 361-369.

(21) Rai, M.; Rahmany, S.; Lim, S. S.; Magdassi, S.; Wong, L. H.; Etgar, L. Hot Dipping Post Treatment for Improved Efficiency in Micro Patterned Semi-Transparent Perovskite Solar Cells. *J. Mater. Chem. A.* **2018**, *6* (46), 23787-23796.

(22) Steirer, K.; Schulz, P.; Teeter, G.; Stevanovic, V.; Yang, M.; Zhu, K.; Berry, J. Defect Tolerance in Methylammonium Lead Triiodide Perovskite. *ACS Energy Lett.* **2016**, *1*(2), 360–366.

(23) Meggiolaro, D.; Motti, S. G.; Mosconi, E.; Barker, A. J.; Ball, J.; Andrea Riccardo Perini, C.; Deschler, F.; Petrozza, A.; De Angelis, F. Iodine Chemistry Determines The Defect Tolerance of Lead-Halide Perovskites. *Energy Environ. Sci.* **2018**, *11* (3), 702-713.

(24) Chen, B.-X.; Rao, H.-S.; Chen, H.-Y.; Li, W.-G.; Kuang, D.-B.; Su, C.-Y. Ordered Macroporous $CH_3NH_3PbI_3$ Perovskite Semitransparent Film for High-Performance Solar Cells. *J. Mater. Chem. A.* **2016**, *4* (40), 15662-15669.

(25) Zhao, L.; Lee, K. M.; Roh, K.; Khan, S. U. Z.; Rand, B. P. Improved Outcoupling Efficiency and Stability of Perovskite Light-Emitting Diodes using Thin Emitting Layers. *Adv. Mater.* **2019**, *31* (2), 1805836.

(26) Prathapani, S.; Bhargava, P.; Mallick, S. Electronic Band Structure and Carrier Concentration of Formamidinium–Cesium Mixed Cation Lead Mixed Halide Hybrid Perovskites. *Appl. Phys. Lett.* **2018**, *112* (9), 092104.

(27) Piper, W. W.; Williams, F. E. Theory of Electroluminescence. *Phys. Rev.* **1955**, *98* (6), 1809-1813.

(28) Watthage, S. C.; Song, Z.; Shrestha, N.; Phillips, A. B.; Liyanage, G. K.; Roland, P. J.; Ellingson, R. J.; Heben, M. J. Enhanced Grain Size, Photoluminescence, and Photoconversion Efficiency with Cadmium Addition during the Two-Step Growth of $CH_3NH_3PbI_3$. *ACS Appl. Mater. Interfaces.* **2017**, *9* (3), 2334-2341.

(29) Kirchartz, T.; Márquez, J. A.; Stolterfoht, M.; Unold, T. Photoluminescence-Based Characterization of Halide Perovskites for Photovoltaics. *Adv. Energy Mater.* **2020**, *10* (26), 1904134.

(30) Gegevičius, R.; Franckevičius, M.; Chmeliov, J.; Tress, W.; Gulbinas, V. Electroluminescence Dynamics in Perovskite Solar Cells Reveals Giant Overshoot Effect. *J. Phys. Chem. Lett.* **2019**, *10* (8), 1779-1783.

(31) Jaramillo-Quintero, O. A.; Sanchez, R. S.; Rincon, M.; Mora-Sero, I. Bright Visible-Infrared Light Emitting Diodes Based on Hybrid Halide Perovskite with Spiro-OMeTAD as a Hole-Injecting Layer. *J. Phys. Chem. Lett.* **2015**, *6* (10), 1883-1890.

(32) Tress, W.; Yavari, M.; Domanski, K.; Yadav, P.; Niesen, B.; Correa Baena, J. P.; Hagfeldt, A.; Graetzel, M. Interpretation and Evolution of Open-Circuit Voltage, Recombination, Ideality Factor and Subgap Defect States during Reversible Light-Soaking and Irreversible Degradation of Perovskite Solar Cells. *Energy Environ. Sci.* **2018**, *11* (1), 151-165.

(33) Marinova, N.; Tress, W.; Humphry-Baker, R.; Dar, M. I.; Bojinov, V.; Zakeeruddin, S. M.; Nazeeruddin, M. K.; Grätzel, M. Light Harvesting and Charge Recombination in $CH_3NH_3PbI_3$ Perovskite Solar Cells Studied by Hole Transport Layer Thickness Variation. *ACS Nano.* **2015**, *9* (4), 4200-4209.

(34) Calado, P.; Burkitt, D.; Yao, J.; Troughton, J.; Watson, T. M.; Carnie, M. J.; Telford, A. M.; O'Regan, B. C.; Nelson, J.; Barnes, P. R. F. Identifying Dominant Recombination Mechanisms in Perovskite Solar Cells by Measuring the Transient Ideality Factor. *Phys. Rev. Appl.* **2019**, *11* (4), 044005.

(35) Jiang, Q.; Zhao, Y.; Zhang, X.; Yang, X.; Chen, Y.; Chu, Z.; Ye, Q.; Li, X.; Yin, Z.; You, J. Surface Passivation of Perovskite Film for Efficient Solar Cells. *Nat. Photonics.* **2019**, *13* (7), 460-466.